Biochemical Journal (2018) **475** 1385–1396
https://doi.org/10.1042/BCJ20170894

Research Article

CGA-N12, a peptide derived from chromogranin A, promotes apoptosis of *Candida tropicalis* by attenuating mitochondrial functions

Ruifang Li, Ruiling Zhang, Yanhui Yang, Xueqin Wang, Yanjie Yi, Pei Fan, Zhengwei Liu, Chen Chen and Junpeng Chang

College of Biological Engineering, Henan University of Technology, Zhengzhou 450001, China

Correspondence: Ruifang Li (lrf@haut.edu.cn)

CGA-N12 (the amino acid sequence from the 65th to the 76th residue of the N-terminus of chromagranin A) is an antifungal peptide derived from human chromogranin A (CGA). In our previous investigation, CGA-N12 was found to have specific anti-candidal activity, though the mechanism of action remained unclear. Here, we investigated the effects of CGA-N12 on mitochondria. We found that CGA-N12 induced an over-generation of intracellular reactive oxygen species and dissipation in mitochondrial membrane potential, in which the former plays key roles in the initiation of apoptosis and the latter is a sign of the cell apoptosis. Accordingly, we assessed the apoptosis features of *Candida tropicalis* cells after treatment with CGA-N12 and found the following: leakage of cytochrome *c* and uptake of calcium ions into mitochondria and the cytosol; metacaspase activation; and apoptotic phenotypes, such as chromatin condensation and DNA degradation. In conclusion, CGA-N12 is capable of inducing apoptosis in *C. tropicalis* cells through mitochondrial dysfunction and metacaspase activation. Antifungal peptide CGA-N12 from human CGA exhibits a novel apoptotic mechanism as an antifungal agent.

Introduction

Azole drugs are commonly used to treat *Candida* infections [1]. However, the misuse of azole compounds in past decades has promoted the emergence of drug-resistant *Candida* species. Moreover, *Candida krusei* exhibits intrinsic resistance to fluconazole. *C. krusei* has been described as a causative agent of disseminated fungal infections in susceptible patients. Although its prevalence remains low among yeast infections (2–5%), its intrinsic resistance to fluconazole makes this yeast important from epidemiologic aspects [2,3]. Thus, novel anti-candidal agents for azole drug-resistant *Candida* species and those that are prone to evoke species resistance are urgently needed [4,5]. One promising source includes antimicrobial peptides (AMPs), which are produced by virtually all life forms as a defense mechanism against competing microbes and represent almost an inexhaustible source of potential therapeutic agents [4–7]. Indeed, AMPs are powerful, multidimensional defense molecules that are not easily overcame by microorganisms using single-approach resistance strategies. For example, many AMPs act by forming pores in microbial membranes, and it appears to be more difficult for microbes to circumvent this generic mode than the specific metabolic-targeting modes of antibiotics [7].

Chromogranin A (CGA) is a soluble protein existed in most endocrine cells and neurons. The N-terminal region of CGA was reported to have antimicrobial activities [8]. In our previous work, the antifungal activity of different derivatives of CGA N-terminus was investigated. CGA-N46 (the amino acid sequence from the 31st to the 76th residue of the N-terminus of chromagranin A), corresponding to the N-terminal Pro31-Gln76 sequence of human CGA, was found to have antagonistic activity against *Candida* species [9]. In ensuing research on the physico-chemical properties of CGA-N46 and

Received: 25 November 2017
Revised: 14 March 2018
Accepted: 20 March 2018

Accepted Manuscript online: 20 March 2018
Version of Record published: 16 April 2018

Biochemical Journal (2018) 475 1385–1396
https://doi.org/10.1042/BCJ20170894

its derivatives, we obtained the more effective derivative CGA-N12 (the amino acid sequence from the 65th to the 76th residue of the N-terminus of chromagranin A), which corresponds to the C-terminus of CGA-N46 and the N-terminal Ala55–Gln76 sequence of human CGA. It shares the structural property and physicochemical characters with CGA-N46 [10]. Compared with its mother peptide, CGA-N12 is more stable and has higher antifungal activity and less hemolytic activity [10]. Our previous reports indicated that CGA-N46 decreases mitochondrial potential [11], an event that occurs in the early stage of apoptosis and plays a key role in this process [12]. We therefore predicted that CGA-N12 inhibits the growth of *Candida* species by promoting apoptosis.

Apoptosis in mammalian cells has been defined as a highly conservative form of programmed cell death (PCD). Although it has been debated for decades whether yeasts undergo apoptosis, i.e. since the first description of yeast apoptosis [13,14], increasing evidence showed that apoptosis is part of the yeast life cycle [15–18]. Two major apoptotic pathways have been described, namely the intrinsic pathway and the extrinsic pathway [19]. Mitochondria play a vital role in the former, which involves apoptotic factors such as cytochrome *c* (Cyt *c*), reactive oxygen species (ROS), intra-mitochondrial calcium ion (Ca^{2+}) homeostasis, and mitochondrial membrane potential [19,20]. Cellular ROS accumulation leads to the opening of mitochondrial permeability transition pores (mPTPs) [16], which result in Cyt *c* leakage and a decrease in mitochondrial potential [12]. In mammalian cells, caspases, which can be activated by mitochondrial-released Cyt *c*, participate in PCD and induce cell death. However, only caspase-like proteases, named metacaspases, are found in plants, fungi, and protozoa [21,22]. Nuclear DNA breakage and chromatin condensation generally occur at the late stage of apoptosis [23].

In the present study, the mechanism related to apoptosis in *Candida* of CGA-N12 was explored by investigating *Candida tropicalis* mitochondrial potential, intracellular ROS accumulation, changes in mitochondrial Cyt *c* and Ca^{2+} (calcium ion) contents, and metacaspase activation, along with apoptotic phenotypes of cells under the effect of CGA-N12.

Materials and methods

Microorganism and materials

C. tropicalis ATCC201381 was supplied by American Type Culture Collection (ATCC; VA, U.S.A.), cultured on Sabouraud dextrose [4% (w/v) glucose and 1% (w/v) peptone], and maintained at 4°C for short-term storage.

CGA-N12 was synthesized by the solid-phase peptide synthesis method with N-terminal and C-terminal de-protection. Peptide purification was performed by high-performance liquid chromatography, and the mass of the peptide was confirmed by mass spectrometry. The anti-candidal activity of CGA-N12 was assessed by the broth micro-dilution method [9]. Other chemicals used in the present study were of analytical grade from commercial suppliers.

Assessment of intracellular ROS accumulation

Intracellular ROS accumulation was detected by dihydrorhodamine-123 (DHR123), an oxidation-sensitive fluorescent dye [24]. Briefly, mid-log-phase *C. tropicalis* cells [1×10^6 CFU (colony-forming unit)] were treated with 75 μM CGA-N12 for 10 h at 28°C. The cells were washed with 20 mM phosphate-buffered saline (PBS; pH 7.0) and stained with 10 μM DHR123 (Sigma–Aldrich, Shanghai, China) for 2 h at 28°C. The samples were analyzed by using a FACSCalibur flow cytometer (BD, U.S.A.). *C. tropicalis* cells not treated with CGA-N12 were used as a negative control, and 10 mM H_2O_2 was used as a positive control. Data represent the mean ± standard deviation for three independent experiments. Statistical significance was determined by Student's *t*-test. *P*-values <0.05 and <0.01 indicate statistical significance.

Assay of mitochondrial membrane potential

In normal cells with polarized mitochondria, the lipophilic cationic dye JC-1 (5,5′,6,6′-tetrachloro-1,1′,3,3′-tetraethyl-imidacarbocyanine) exists as aggregates (red fluorescence, 595 nm); in apoptotic cells with mitochondrial membrane potential dissipation, mitochondrial depolarization leads to the formation of JC-1 monomers (green fluorescence, 525 nm) [18]. The ratio of aggregates to monomers reflects changes in mitochondrial membrane potential. Molecular probes JC-1 (Beyotime, Shanghai, China) was used to examine the effect of CGA-N12 on the mitochondrial membrane potential of *C. tropicalis* cells, as recently described [18]. Fluorescence of aggregates and monomers was detected by flow cytometry. Briefly, log-phase *C. tropicalis* cells

(1×10^6 CFU) were treated with 75 μM CGA-N12 at 28°C for 10 h. The cells were washed and resuspended in 20 mM PBS (pH 7.0); 1 × JC-1 was added to a final concentration of 2.5 μg/ml, and the mixture was incubated at 28°C for 30 min. The mean fluorescence intensity at 525 or 595 nm was recorded with a FACSCalibur flow cytometer (BD, U.S.A.). *C. tropicalis* cells not treated with CGA-N12 were used as a negative control, and 10 mM H_2O_2 was used as a positive control. The ratio of JC-1 aggregate to monomer intensity was calculated, and the data represent the mean ± standard deviation for three independent experiments. Statistical significance was determined by Student's *t*-test. *P*-values <0.05 and <0.01 indicate statistical significance.

Preparation of calcein-loaded liposomes

Calcein-loaded liposomes were prepared according to a reported method [25]. Phosphatidylcholine and cholesterol (10 : 1, w/w) were obtained from Sigma–Aldrich (Shanghai, China) and employed to mimic eukaryote cell membranes. The material was first dissolved in chloroform, and the organic solvent was then completely evaporated using a rotary vacuum evaporator at 50°C, resulting in a thin film on the sides of a round-bottomed flask. The dried film was rehydrated with calcein solution (90 mM calcein, 20 mM PBS; pH 7.0), and the mixture was ultrasonicated at 400 W for 15 min and extruded through 0.22-μm pore-size polycarbonate membranes. Free calcein was removed using a Sephadex G-50 column.

Assay of calcein leakage

A suspension of liposomes containing calcein was treated with 75 μM CGA-N12 at 28°C to evaluate CGA-N12-mediated disruption of membrane integrity by measuring calcein leakage [25]. The dye release from liposomes was assessed by measuring fluorescence intensities (Ex. 490 nm, Em. 517 nm) every 0.5 h with a fluorescence spectrophotometer (Cary Eclipse, Australia). For this assay, 20 mM PBS (pH 7.0) was selected as a negative control, and 10 mM H_2O_2 was used as a positive control. All samples were examined three times. One hundred percent dye release from liposomes at 10 h was obtained with the addition of 0.1% Triton X-100 in Tris buffer.

Detection of cytochrome *c* release

CGA-N12-mediated changes in the Cyt *c* content of mitochondria and the cytosol at different times was analyzed to estimate Cyt *c* release from mitochondria to the cytosol via differential velocity centrifugation [18]. Briefly, *C. tropicalis* cells were incubated with 75 μM CGA-N12 for 0, 5, 10, and 15 h at 28°C. The incubated cells were homogenously dispersed in medium [50 mM Tris, 2 mM ethylenediaminetetraacetic acid (EDTA), 1 mM phenylmethanesulfonyl fluoride; pH 7.5] and then 2% glucose was added. The mixture was centrifuged at 20 000×***g*** for 10 min, and both the supernatant and cell pellet were collected. The supernatant was centrifuged by superspeed centrifugation (CP-100WX; Hitachi, Japan) at 305 000×***g*** for 45 min, and the resulting supernatant from the superspeed centrifugation was collected for quantification of cytosolic Cyt *c*. To quantify mitochondrial Cyt *c*, the cell pellets obtained from centrifugation at 20 000×***g*** in the above step were homogenized in Tris–EDTA buffer (50 mM Tris, 2 mM EDTA; pH 5.0) and centrifuged at 7727×***g*** for 30 s. The resulting pellet was suspended in 2 mg/ml Tris–EDTA buffer (2 mg/ml Tris, 2 mM EDTA; pH 5.0). Ascorbic acid was added to a final concentration of 500 mg/ml for 5 min to reduce Cyt *c* in cytosolic sample and mitochondrial sample. The absorbance at 550 nm was measured with a spectrophotometer (UV1800; AOXI, Shanghai, China) to determine the relative quantities of reduced cytoplasmic Cyt *c* and mitochondrial Cyt *c* in the samples.

Data are presented as the mean ± standard deviation from three independent experiments. Statistical significance was determined by Student's *t*-test. *P*-values <0.05 and <0.01 indicate statistical significance.

Detection of calcium ion uptake

To elucidate Ca^{2+} uptake under the effect of CGA-N12, Ca^{2+} probes Fura-2-AM and Rhod-2-AM (Sigma–Aldrich, Shanghai, China) were used to detect changes in the Ca^{2+} content of the cytosol and mitochondria, respectively [18]. For specific experimental steps, refer to Heejeong Lee's research [26]. *C. tropicalis* cells (1×10^6) were incubated with 75 μM CGA-N12 for 0, 5, 10 and 15 h at 28°C; 10 mM H_2O_2 was used as a positive control. The cells were washed with Krebs buffer (132 mM NaCl, 4 mM KCl, 1.4 mM $MgCl_2$, 6 mM glucose, 10 mM HEPES, 10 mM $NaHCO_3$, and 1 mM $CaCl_2$; pH 7.2) containing 0.01% Pluronic F-127 (Sigma–Aldrich, Shanghai, China) and 1% bovine serum albumin. The suspensions were incubated with 5 μM Fura-2-AM or 10 μM Rhod-2-AM at 28°C for 30 min. Three washes were performed with calcium-free Krebs buffer.

Biochemical Journal (2018) 475 1385–1396
https://doi.org/10.1042/BCJ20170894

Fura-2-AM and Rhod-2-AM were detected at Ex/Em = 340 nm/510 nm and Ex/Em = 550 nm/580 nm, respectively, using a fluorescence spectrophotometer (Cary Eclipse, Australia).

Detection of metacaspase activity

Activation of *Candida* metacaspase was measured using the CaspACETM FITC-VAD-FMK *In Situ* Marker (Sigma–Aldrich, Shanghai, China), a general caspase inhibitor, according to a recently described method [26]. Briefly, *C. tropicalis* cells (1×10^6) were treated with 75 μM CGA-N12 at 28°C for 10 h. The cells were then washed and stained with 2.5 μM CaspACE FITC-VAD-FMK *In Situ* Marker at 28°C for 30 min. The fluorescence intensity was evaluated using a fluorescence spectrophotometer (Cary Eclipse, Australia). *C. tropicalis* cells that had not undergone CGA-N12 treatment were used as a negative control, and melittin was used as a positive control.

Detection of nuclear condensation

Nuclear condensation was examined by 4,6-diamidino-2-phenylindole (DAPI) staining (Sigma–Aldrich, Shanghai, China) [26]. *C. tropicalis* cells (1×10^6) in log phase were treated with 75 μM CGA-N12 for 10 h at 28°C. The cells were washed and then stained with DAPI (40 μg/ml) for 30 min. After washing, the samples were observed using a laser scanning confocal microscope (Olympus FA100, U.S.A.). *C. tropicalis* cells that had not undergone CGA-N12 treatment were used as a control.

Detection of DNA fragments

Nuclear fragments were examined by agarose gel electrophoresis [27]. Briefly, log-phase *C. tropicalis* cells were treated with 75 μM CGA-N12 at 28°C for 0, 5, 10, 15, 20 and 25 h, harvested by centrifugation, and washed with 20 mM PBS (pH 7.0). Approximately 0.1 g of cells (wet weight) were lysed with 1 ml of fresh lysis buffer [180 mM EDTA (pH 8.0), 50 mM Tris–HCl (pH 8.0), 0.5 M NaCl, and 1% sodium dodecyl sulfate] with 0.3 volume of quartz in the Eppendorf tube. After vortexing for 10 min, the samples were incubated for 30 min at 65°C. Approximately 600 μl of 7.5 M ammonium acetate solution was added, and the samples were placed in an ice bath for 10 min. After centrifugation, the chromosomal DNA in the supernatant was precipitated with the addition of isopropyl alcohol. This crude extraction of DNA was incubated with 10 μl of DNase-free RNase (100 μg/ml) and 20 μl of protease K (10 mg/l) for 1 h at 37°C and then resuspended in 50 μl of TE buffer. This extract was added to 10 μl 6× loading buffer containing nucleic acid dye Goldview I and electrophoresed through a 2% agarose gel at 50 V for 30 min.

Results

CGA-N12 induces ROS accumulation

ROS participate in many significant biochemical processes, though ROS over-generation causes mitochondrial dysfunction and induces apoptosis [16,28]. In our study, the level of ROS in *C. tropicalis* cells treated with CGA-N12 was evaluated by assessing DHR123 florescence intensity, whereby an increase in DHR123 intensity can be interpreted as an increase in ROS production. The fluorescence of CGA-N12- or H_2O_2-treated cells increased by 30.5% or 78.7%, respectively, compared with the negative control (Figure 1). These results indicate that CGA-N12 induced ROS accumulation in *C. tropicalis* cells. Therefore, CGA-N12 promotes apoptosis in yeast cells by inducing ROS accumulation.

Effect of CGA-N12 on mitochondrial membrane potential

The mitochondrial membrane potential is a key indicator of mitochondrial function, and a dissipation in mitochondrial membrane potential is a sign of early apoptosis [12]. In our study, JC-1 was used to examine mitochondrial membrane potential, and the fluorescence of JC-1 aggregates (FL2) and monomers (FL1) was detected by flow cytometry; the ratio of red (FL2) to green (FL1) fluorescence was calculated, and a decrease in this ratio was interpreted as mitochondrial depolarization. The fluorescence ratios of FL2/FL1 in cells treated with CGA-N12 and H_2O_2 were 0.88 and 0.38, respectively, which were lower than that (1.74) of the control cells (Figure 2). These results indicate that CGA-N12 induces mitochondrial depolarization in cells undergoing apoptosis.

Biochemical Journal (2018) **475** 1385–1396
https://doi.org/10.1042/BCJ20170894

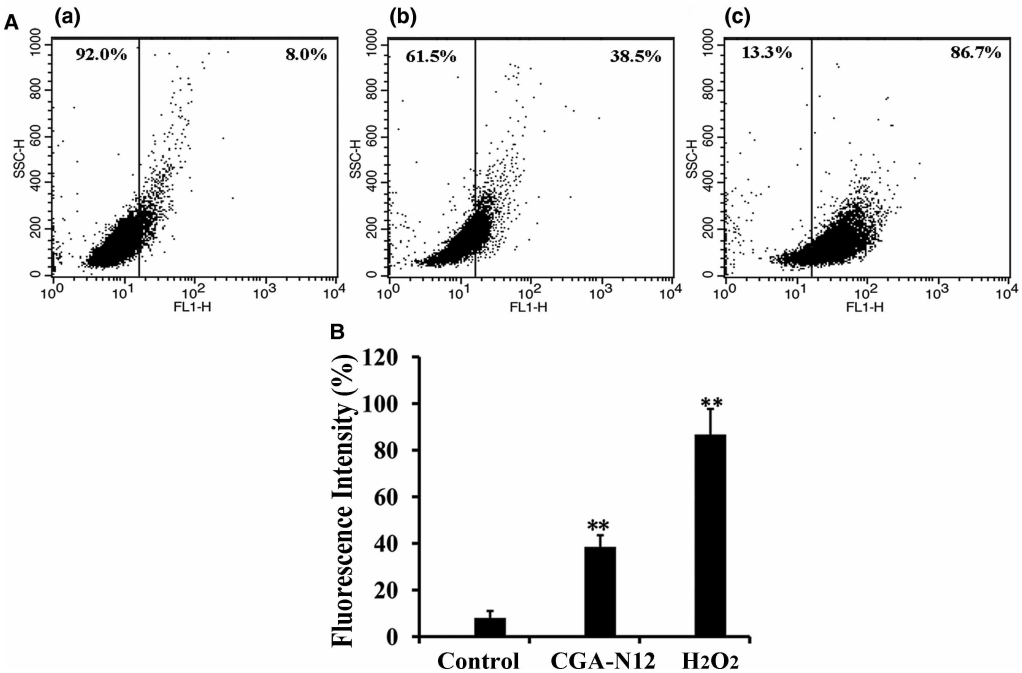

Figure 1. Detection of the effect of CGA-N12 on intracellular ROS accumulation.

(**A**) Approximately 1 × 10^6 *C. tropicalis* cells were incubated with 75 μM CGA-N12 or 10 mM H_2O_2 for 10 h at 28°C. Intracellular ROS levels were detected by flow cytometry using dihydrorhodamine-123. Increases in fluorescence intensity indicate higher ROS levels. (a) Control cells that did not undergo CGA-N12 treatment; (b) cells exposed to 75 μM CGA-N12; (c) cells exposed to 10 mM H_2O_2. (**B**) Data represent the mean ± standard deviation for three independent experiments. Statistical significance was determined by Student's *t*-test. ** indicates statistical significant difference (*P*-values <0.01).

Effect of CGA-N12 on membrane integrity

To determine whether pores can be formed in the fungal membrane, membrane disruption was investigated by examining calcein release from liposomes treated with CGA-N12. The results showed that exposure to CGA-N12 did not cause the calcein encased in liposomes to leak (Figure 3), which indicated that CGA-N12 cannot disrupt the bilayer of neutral liposomes. In contrast, complete leakage from liposomes was observed at 10 h after the addition of the membrane-disrupting agent Triton X-100.

Release of cytochrome *c* from mitochondria

Apoptosis is often caused by release of the apoptosis-promoting factor Cyt *c* from mitochondria into the cytosol [29]. Mitochondrial Cyt *c* is closely associated with the inner mitochondrial membrane, though it can be released into the cytosol when mPTPs of the outer membrane are open [30]. At 10 h after the treatment of *C. tropicalis* cells with CGA-N12, Cyt *c* levels increased in the cytoplasm and decreased in mitochondria compared with the control (Figure 4). The results show that CGA-N12 induces Cyt *c* release from mitochondria to the cytoplasm after 10 h of treatment, which will active caspases to promote apoptosis.

Effect on cytosolic and mitochondrial calcium ion levels

Calcium is a key regulator of mitochondrial function and acts at several levels within the organelle to stimulate ATP synthesis [31]. Increases in cytosolic and mitochondrial Ca^{2+} levels induce ROS accumulation, and eliciting an increase in mitochondrial membrane permeability, and the dysregulation of mitochondrial Ca^{2+} homeostasis is now recognized to play a key role in several pathologies [31,32]. The Ca^{2+}-sensitive fluorescent dyes Fura-2-AM (cytoplasm) and Rhod-2-AM (mitochondria) were employed to measure changes of Ca^{2+} contents in the cytosol and mitochondria, respectively, after treatment with CGA-N12. Compared with the control, Ca^{2+} levels in cytosolic and mitochondria were notably increased after treatment with CGA-N12 for 10 h (Figure 5), indicating that CGA-N12 induces an influx of Ca^{2+} into cells to disrupt mitochondrial and cytosolic Ca^{2+}

Biochemical Journal (2018) **475** 1385–1396
https://doi.org/10.1042/BCJ20170894

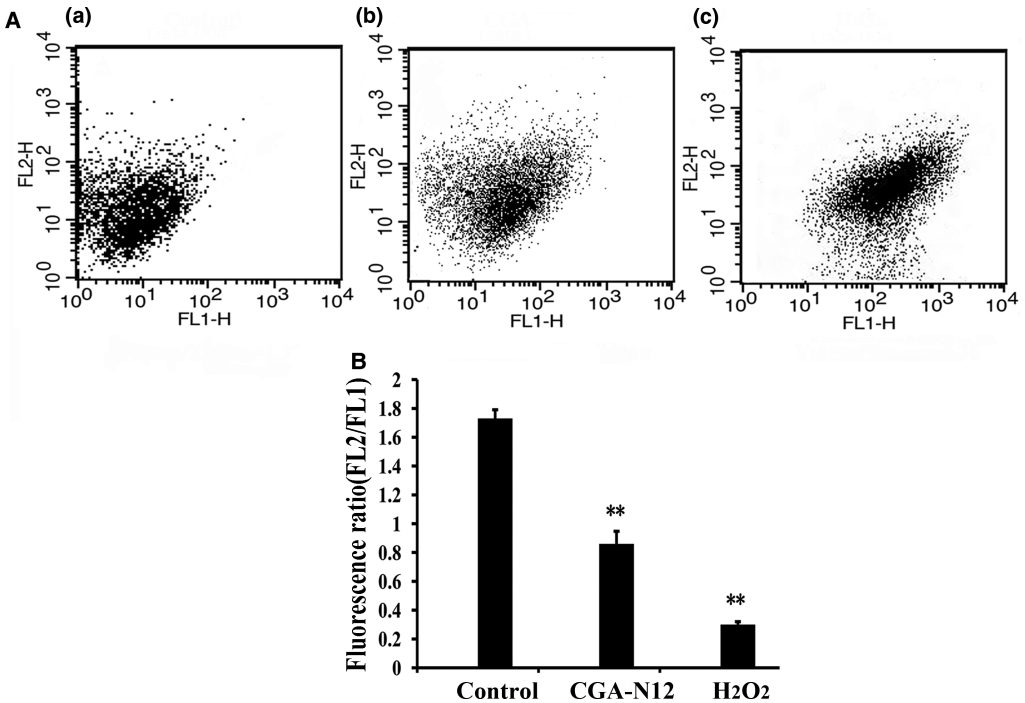

Figure 2. Detection of the effect of CGA-N12 on mitochondrial membrane potential.

(**A**) Approximately 1×10^6 *C. tropicalis* cells were incubated with 75 μM CGA-N12 or 10 mM H_2O_2 for 10 h at 28°C; mitochondrial membrane potential levels were detected by flow cytometry using JC-1. A decrease in the ratio of FL2 to FL1 was interpreted as mitochondrial depolarization. (a) Control cells that had not undergone CGA-N12 treatment; (b) cells exposed to 75 μM CGA-N12; (c) cells exposed to 10 mM H_2O_2. (**B**) Data represent the mean ± standard deviation for three independent experiments. Statistical significance was determined by Student's *t*-test. ** indicates statistical significant difference (*P*-values <0.01).

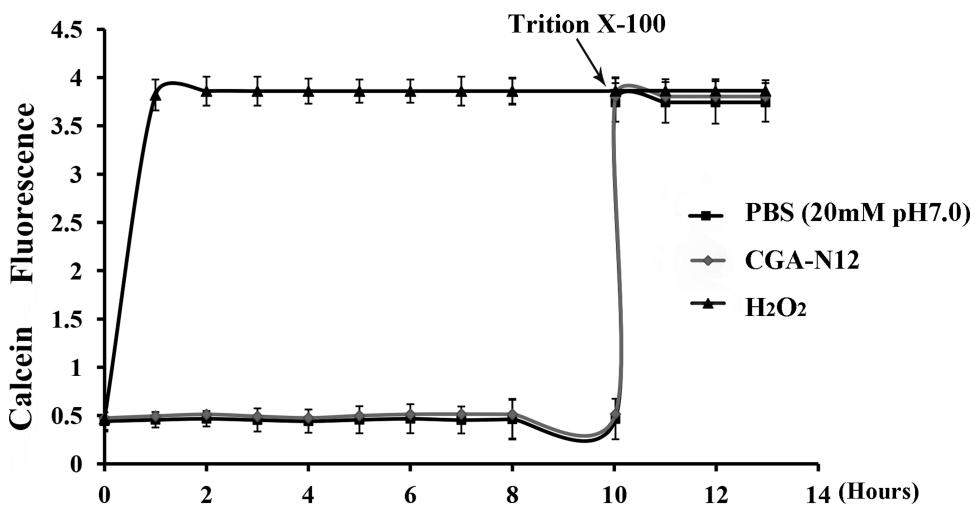

Figure 3. Detection of the effect of CGA-N12 on liposome permeability.

Calcein-loaded liposomes were incubated with 75 μM CGA-N12 or 10 mM H_2O_2 at 28°C. Fluorescence of calcium released from the liposomes was recorded using a fluorescence spectrophotometer; an increase in fluorescence was interpreted as an increase in membrane permeability. Complete leakage from liposomes was observed upon the addition of the membrane-disrupting agent Triton X-100 at 10 h. Data represent the mean ± standard deviation for three independent experiments.

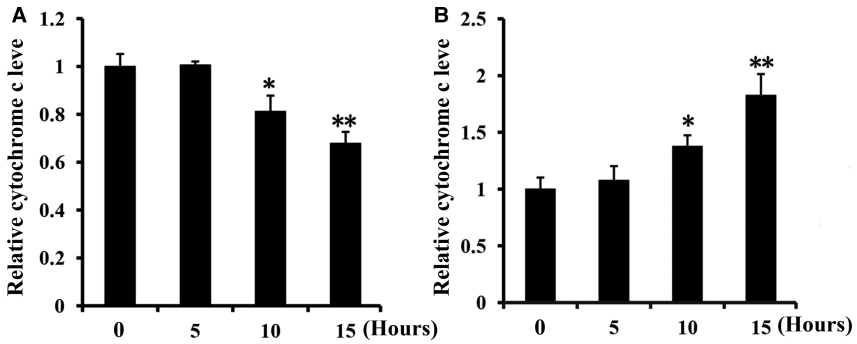

Figure 4. Detection of the effect of CGA-N12 on mitochondrial Cyt *c* leakage.

C. tropicalis cells were incubated with 75 μM CGA-N12 for 0, 5, 10, and 15 h at 28°C. The Cyt *c* contents in mitochondria and the cytoplasm were detected by measuring absorbance at 550 nm. Relative levels of (**A**) mitochondrial Cyt *c* and (**B**) cytoplasmic Cyt *c*. Data represent the mean ± standard deviation for three independent experiments. Statistical significance was determined by Student's *t*-test. ** indicates statistical significant difference (*P*-values <0.01).

homeostasis. The increased cytosolic Ca^{2+} and ROS generation initiates yeast apoptosis by triggering mitochondrial permeabilization and release of proapoptotic factors.

Metacaspase activation

Loss of mitochondrial membrane potential is considered a hallmark of the early stage of the apoptosis pathway, and this event coincides with caspase activation [32]. To assess metacaspase activity, we utilized CaspACE™ FITC-VAD-FMK *In Situ* Marker, a fluorescent analog of the caspase inhibitor Z-VAD-FMK. The fluorescein isothiocyanate (FITC) group replaces the carbonyl group (Z) in the N-terminal blocking group to produce a fluorescent apoptotic standard, and this structure allows the caspase inhibitor to enter a cell and irreversibly bind to activated caspases *in situ*; caspase activity is then detected *in situ* by green fluorescence. Compared with the control, the fluorescence of CGA-N12-treated cells increased by 30.11% (Figure 6), demonstrating that CGA-N12 triggers metacaspase activity. The activated metacaspase leads the cells into caspase-dependent apoptosis.

Effect of CGA-N12 on apoptotic phenotypes

Chromatin condensation and DNA fragmentation occur in the late period of apoptosis and are used as key markers of the process [33]. In this study, DAPI, which is able to bind to AT sites within the minor groove of

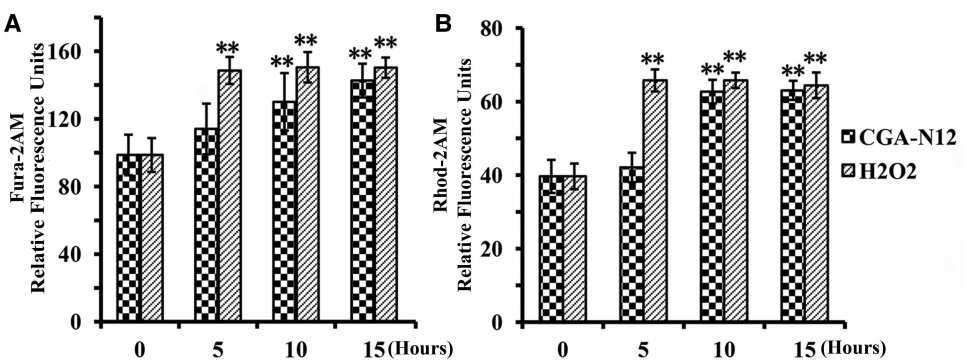

Figure 5. Detection of the effect of CGA-N12 on mitochondrial calcium ion influx.

Approximately 1×10^6 *C. tropicalis* cells were incubated with 75 μM CGA-N12 at 28°C for 0, 5, 10, and 15 h. The fluorescence intensity of cytosolic and mitochondrial Ca^{2+} levels was assessed using Fura-2-AM (Ex/Em = 340 nm/510 nm) and Rhod-2-AM (Ex/Em = 550 nm/580 nm), respectively. Relative levels of (**A**) cytoplasmic calcium ion and (**B**) mitochondrial calcium ion. Data represent the mean ± standard deviation for three independent experiments. Statistical significance was determined by Student's *t*-test. ** indicates statistical significant difference (*P*-values <0.01).

Biochemical Journal (2018) **475** 1385–1396
https://doi.org/10.1042/BCJ20170894

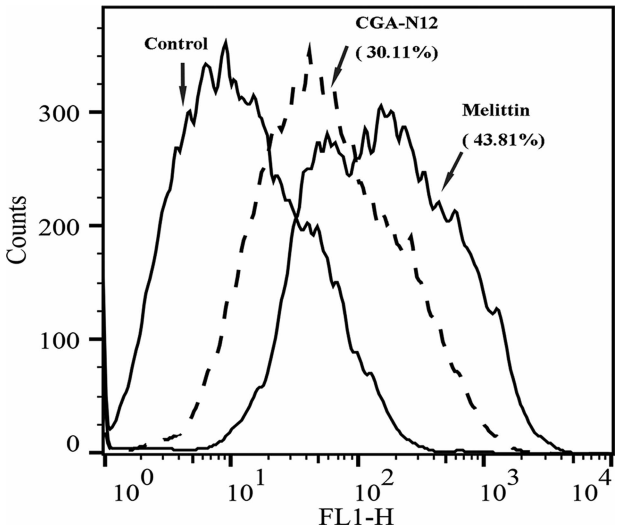

Figure 6. Detection of the effect of CGA-N12 on intracellular metacaspase activation.

Metacaspase activity in *C. tropicalis* cells was confirmed using CaspACE™ FITC-VAD-FMK *In Situ* Marker staining with flow cytometry. *C. tropicalis* cells (1×10^6) were incubated with 75 μM CGA-N12 and 10 mM H_2O_2 at 28°C for 10 h.

DNA [24], was used to assay chromatin condensation. Compared with untreated cells, cells treated with CGA-N12 exhibited chromatin condensation (Figure 7A). Agarose gel electrophoresis was also performed to assess whether CGA-N12 affects the integrity of yeast DNA. After treatment with CGA-N12, chromosomal DNA was degraded into fragments of approximately integer multiples of 100 bp (Figure 7B), revealing a typical DNA 'ladder'. These results demonstrate an apoptotic phenotype in *C. tropicalis* cells.

Discussion

In the present study, we found that CGA-N12 did not perturb the plasma membrane, i.e. CGA-N12 is different from a membrane-active peptide [34–38]. Accordingly, we examined the intracellular responses of CGA-N12,

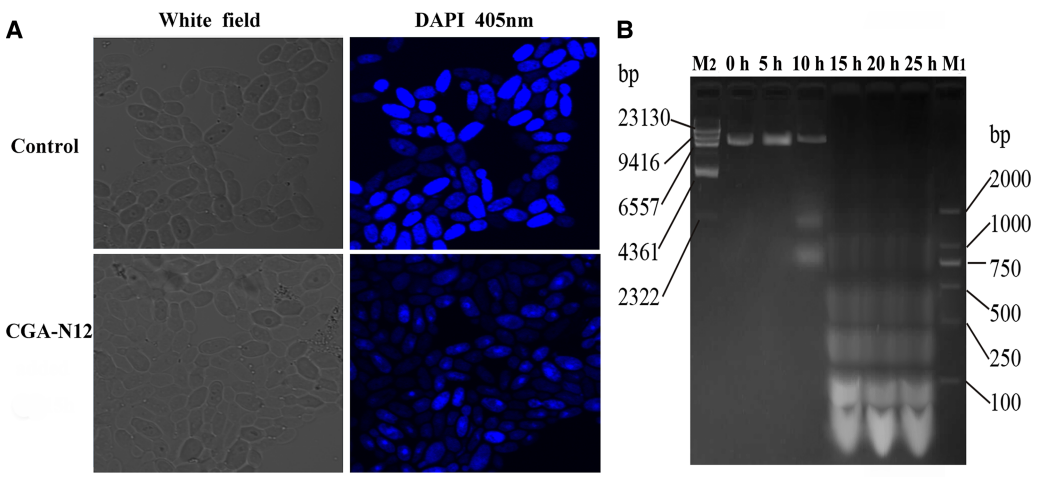

Figure 7. Detection of the apoptotic phenotypes of *C. tropicalis* cells under the effect of CGA-N12.

(**A**) Approximately 1×10^6 *C. tropicalis* cells in log phase were treated with 75 μM CGA-N12 for 10 h, and chromatin condensation with DAPI staining was visualized by laser scanning confocal microscopy. *C. tropicalis* cells that had not undergone CGA-N12 treatment were used as a control. (**B**) DNA fragmentation was detected by gel electrophoresis. Chromatin from *C. tropicalis* cells after treatment with CGA-N12 for 0, 5, 10, 15, 20, and 25 h at 28°C was examined by gel electrophoresis. M1 and M2 are molecular mass standards.

which was found to induce ROS accumulation and a dissipation in mitochondrial potential. In addition, CGA-N12 promoted cytosolic and mitochondrial Ca^{2+} uptake, Cyt *c* release, and metacaspase activation as well as nuclear condensation and DNA fragmentation.

Mitochondrial dysfunction has been shown to participate in the induction of apoptosis and even been the central of the apoptotic pathway. Membrane potential is a key to maintaining mitochondrial function [12]. There are emerging data, suggesting that the loss of mitochondrial potential may be a consequence of the apoptotic-signaling pathway [39]. In our research, after the treatment of CGA-N12, a dissipation of the mitochondrial membrane potential appeared.

Apoptosis is associated in many cases with the generation of ROS in cells across a wide range of organisms including lower eukaryotes such as the yeast *Saccharomyces cerevisiae* [28]. Oxidative stress is linked to the level of Ca^{2+}, which plays a significant role in the regulation of cellular processes [32]. In addition, mitochondrial ROS production is closely related to mitochondrial Ca^{2+} homeostasis [31,32]. Conversely, mitochondrial matrix Ca^{2+} overload also can lead to enhanced generation of ROS [31]. With many stimuli, increased cytosolic Ca^{2+} and ROS generation are the triggering signals that lead to mitochondrial permeabilization and release of proapoptotic factors, which initiate yeast PCD [31,32]. In this study, CGA-N12 induced accumulation of ROS in cells, and cytosolic and mitochondrial Ca^{2+} homeostasis was altered by Ca^{2+} influx. Ca^{2+} uptake induction has also been reported for some AMPs, such as scolopendin, cecropin A, and other antileishmanial agent Allicin, which, inducing Ca^{2+} influx into mitochondria, is a part of the apoptotic phenotype [18,20,24,40].

Endogenous oxidative stress directly leads to the opening of the mPTPs, followed by induction of apoptotic markers in the whole yeast cells [16]. The opening of mPTPs leads to the increase in mitochondrial permeability, causing the release of apoptotic factors, such as Cyt *c*, from mitochondria to the cytoplasm [41]; a decrease in mitochondrial membrane potential then ensues [32,42]. Cyt *c* has been identified as a key signaling molecule of apoptosis; it can initiate the caspase activation cascade once released into the cytosol through interactions with apoptotic protease-activating factors (Apaf) [29]. Two types of Cyt *c* are found in the mitochondrial interior membrane space: one that is free or is weakly associated with the inner phospholipid membrane [43,44] and another that stably binds to the inner mitochondrial membrane via electrostatic interactions and hydrophobic forces [45]. The former type is responsible for mitochondrial respiration, whereas the latter activates apoptosis [46–48]. Although certain studies suggest that Cyt *c* is related to apoptosis in yeast [41,49], it is not clearly understood whether Cyt *c* participates in yeast apoptosis in the same way as it does in mammalian cells [41]. Our results verify that Cyt *c* is released from mitochondria and participates in apoptosis of yeast cells after treatment with CGA-N12.

Two families of caspase-like proteins have been identified: Paracaspases (found in metazoans and Dictyostelium) and metacaspases (found in plants, fungi, and protozoa) [21]. To date, there are no reports of metacaspase involvement in apoptosis of *C. albicans*. However, it has been recognized that the *S. cerevisiae* genome harbors a single metacaspase, YCA1, which has caspase-like activity and has been implicated in yeast apoptosis [22]. Additionally, YCA1 has been associated with apoptosis in yeast cells exposed to H_2O_2 [22]. CaMCA1, a homolog of *S. cerevisiae* metacaspase YCA1, could both attenuated oxidative stress-induced cell death and caspase activation [50]. In our research, metacaspase activation coincided with apoptosis in *C. tropicalis* cells.

In mammalian cells, apoptosis is classified into caspase-dependent and caspase-independent apoptosis [15]. Apoptotic stimuli typically lead to the release of Cyt *c*, ultimately activating caspase. In contrast, metacaspase in yeast cells acts as an executioner, inducing irreversible apoptosis, and Cyt *c* release is not followed by metacaspase activation [32]. CGA-N12 was found to induce Cyt *c* release, caspase activation, and apoptosis in *C. tropicalis* cells. Nonetheless, further research is needed to investigate whether the Cyt *c* released from mitochondria induces metacaspase activation.

Intracellularly accumulated ROS mainly attack the nucleic acids of chromosomes, which result in single- or double-stranded DNA breaks [28,51,52], and DNA fragmentation and nuclear condensation are typical features of late apoptosis. After treatment of CGA-N12, DNA fragmentation and nuclear condensation were also appeared. Therefore, *C. tropicalis* cell death due to CGA-N12 shares many comparable features with yeast apoptosis.

In conclusion, the predicted intracellular mechanism of action of CGA-N12 in *C. tropicalis* cells occurs through induction of intracellular ROS accumulation. Under the condition of oxidation stress, mitochondrial membrane permeability increased, which allowed an efflux of Cyt *c* from mitochondria and an influx of Ca^{2+} into mitochondria, without disturbing membrane integrity and resulting in the dissipation of mitochondrial

Biochemical Journal (2018) **475** 1385–1396
https://doi.org/10.1042/BCJ20170894

membrane potential, which is also a sign of apoptosis. Metacaspases in cytoplasm were activated by Cyt *c* leaked from mitochondria. Metacaspase activation promoted apoptosis, and ROS accumulation further induced nuclear condensation and DNA fragmentation, which represent the late apoptotic phenotype. Therefore, CGA-N12 induced apoptosis in *C. tropicalis* by attenuating mitochondrial function. Further investigation is needed to evaluate whether CGA-N12 induces caspase-dependent apoptosis in yeast.

Abbreviations

AMPs, antimicrobial peptides; ATCC, American Type Culture Collection; Ca^{2+}, calcium ion; CFU, colony-forming unit; CGA, chromagranin A; CGA-N12, the amino acid sequence from the 65th to the 76th residue of the N-terminus of chromagranin A; CGA-N46, the amino acid sequence from the 31st to the 76th residue of the N-terminus of chromagranin A; Cyt *c*, cytochrome *c*; DAPI, 4,6-diamidino-2-phenylindole; DHR123, dihydrorhodamine-123; EDTA, ethylenediaminetetraacetic acid; FITC, fluorescein isothiocyanate; JC-1, 5,5′,6,6′-tetrachloro-1,1′,3,3′-tetraethyl-imidacarbocyanine; mPTP, mitochondrial permeability transition pore; PBS, phosphate-buffered saline; PCD, programmed cell death; ROS, reactive oxygen species.

Author Contribution

R.L. drafted the manuscript and participated in the design and coordination of the experiment. R.Z. carried out the experiments and drafted the manuscript. Y.Ya. and X.W. provided general guidance and participated in the final editing of the manuscript. Y.Y. and P.F. provided guidance for the experiments. Z.L., C.C., and J.C. participated in the experimental design. All authors have read and approved the final manuscript.

Funding

The present study was supported by the National Natural Science Foundation of China [31071922 and 31572264], Fundamental Research Funds for Henan Provincial Colleges and Universities in Henan University of Technology [2015RCJH03], Henan Provincial Science and Technology Research Project [162102310404], and National Engineering Laboratory for Wheat & Corn Further Processing, Henan University of Technology [NL2016010].

Competing Interests

The Authors declare that there are no competing interests associated with the manuscript.

References

1 Chai, L.Y.A., Denning, D.W. and Warn, P. (2010) *Candida tropicalis* in human disease. *Crit. Rev. Microbiol.* **36**, 282–298 https://doi.org/10.3109/1040841X.2010.489506
2 Scorzoni, L., de Lucas, M.P., Mesa-Arango, A.C., Fusco-Almeida, A.M., Lozano, E., Cuenca-Estrella, M. et al. (2013) Antifungal efficacy during *Candida krusei* infection in non-conventional models correlates with the yeast in vitro susceptibility profile. *PLoS ONE* **8**, e60047 https://doi.org/10.1371/journal.pone.0060047
3 Muñoz, P., Sánchez-Somolinos, M., Alcalá, L., Rodríguez-Créixems, M., Peláez, T. and Bouza, E. (2005) *Candida krusei* fungaemia: antifungal susceptibility and clinical presentation of an uncommon entity during 15 years in a single general hospital. *J. Antimicrob. Chemother.* **55**, 188–193 https://doi.org/10.1093/jac/dkh532
4 Yeaman, M.R. and Yount, N.Y. (2003) Mechanisms of antimicrobial peptide action and resistance. *Pharmacol. Rev.* **55**, 27–55 https://doi.org/10.1124/pr.55.1.2
5 Hu, K., Jiang, Y., Xie, Y., Liu, H., Liu, R., Zhao, Z. et al. (2015) Small-anion selective transmembrane “holes” induced by an antimicrobial peptide too short to span membranes. *J. Phys. Chem. B* **119**, 8553–8560 https://doi.org/10.1021/acs.jpcb.5b03133
6 Guaní-guerra, E., Santos-mendoza, T., Lugo-reyes, S.O. and Terán, L.M. (2010) Antimicrobial peptides: general overview and clinical implications in human health and disease. *Clin. Immunol.* **135**, 1–11 https://doi.org/10.1016/j.clim.2009.12.004
7 Wiesner, J. and Vilcinskas, A. (2010) Antimicrobial peptides: the ancient arm of the human immune system. *Virulence* **1**, 440–464 https://doi.org/10.4161/viru.1.5.12983
8 Helman, L.J., Ahn, T.G., Levine, M.A., Allison, A., Cohen, P.S., Cooper, M.J. et al. (1988) Molecular cloning and primary structure of human chromogranin A (secretory protein I) cDNA. *J. Biol. Chem.* **263**, 11559–11563 PMID:3403545
9 Li, R.-F., Lu, Y.-L., Lu, Y.-B., Zhang, H.-R., Huang, L., Yin, Y.-L. et al. (2015) Antiproliferative effect and characterization of a novel antifungal peptide derived from human Chromogranin A. *Exp. Ther. Med.* **10**, 2289–2294 https://doi.org/10.3892/etm.2015.2838
10 Li, R.-F., Lu, Z.-F., Sun, Y.-N., Chen, S.-H., Yi, Y.-J., Zhang, H.-R. et al. (2016) Molecular design, structural analysis and antifungal activity of derivatives of peptide CGA-N46. *Interdiscip. Sci. Comput. Life Sci.* **8**, 319–326 https://doi.org/10.1007/s12539-016-0163-x
11 Li, R.-F., Yan, X.-H., Lu, Y.-L., Lu, Y.-B., Zhang, H.-R., Chen, S.-H. et al. (2015) Anti-candidal activity of a novel peptide derived from human chromogranin A and its mechanism of action against *Candida krusei*. *Exp. Ther. Med.* **10**, 1768–1776 https://doi.org/10.3892/etm.2015.2731
12 Krysko, D.V., Roels, F., Leybaert, L. and D’Herde, K. (2001) Mitochondrial transmembrane potential changes support the concept of mitochondrial heterogeneity during apoptosis. *J. Histochem. Cytochem.* **49**, 1277–1284 https://doi.org/10.1177/002215540104901010

13 Rockenfeller, P. and Madeo, F. (2008) Apoptotic death of ageing yeast. *Exp. Gerontol.* **43**, 876–881 https://doi.org/10.1016/j.exger.2008.08.044
14 Madeo, F., Fröhlich, E. and Fröhlich, K. U. (1997) A yeast mutant showing diagnostic markers of early and late apoptosis. *J. Cell Biol.* **139**, 729–734 PMID:9348289
15 Madeo, F., Carmona-Gutierrez, D., Ring, J., Büttner, S., Eisenberg, T. and Kroemer, G. (2009) Caspase-dependent and caspase-independent cell death pathways in yeast. *Biochem. Biophys. Res. Commun.* **382**, 227–231 https://doi.org/10.1016/j.bbrc.2009.02.117
16 Deryabina, Y., Isakova, E., Antipov, A. and Saris, N.E.L. (2013) The inhibitors of antioxidant cell enzymes induce permeability transition in yeast mitochondria. *J. Bioenerg. Biomembr.* **45**, 491–504 https://doi.org/10.1007/s10863-013-9511-2
17 Liang, Q., Li, W. and Zhou, B. (2008) Caspase-independent apoptosis in yeast. *Biochim. Biophys. Acta, Mol. Cell Res.* **1783**, 1311–1319 https://doi.org/10.1016/j.bbamcr.2008.02.018
18 Lee, H., Hwang, J.-S. and Lee, D.G. (2017) Scolopendin, an antimicrobial peptide from centipede, attenuates mitochondrial functions and triggers apoptosis in *Candida albicans*. *Biochem. J.* **474**, 635–645 https://doi.org/10.1042/BCJ20161039
19 Carmona-Gutierrez, D., Eisenberg, T., Büttner, S., Meisinger, C., Kroemer, G. and Madeo, F. (2010) Apoptosis in yeast: triggers, pathways, subroutines. *Cell Death Differ.* **17**, 763–773 https://doi.org/10.1038/cdd.2009.219
20 Yun, J.E. and Lee, D.G. (2016) Cecropin A-induced apoptosis is regulated by ion balance and glutathione antioxidant system in *Candida albicans*. *IUBMB Life* **68**, 652–662 https://doi.org/10.1002/iub.1527
21 Uren, A.G., O'Rourke, K., Aravind, L., Pisabarro, M.T., Seshagiri, S., Koonin, E.V. et al. (2000) Identification of paracaspases and metacaspases: two ancient families of caspase-like proteins, one of which plays a key role in MALT lymphoma. *Mol. Cell* **6**, 961–967 https://doi.org/10.1016/S1097-2765(00)00094-0
22 Madeo, F., Herker, E., Maldener, C., Wissing, S., Lächelt, S., Herlan, M. et al. 2002. A caspase-related protease regulates apoptosis in yeast. *Mol. Cell* **9**, 911–917 PMID:11983181
23 Dobrucki, J. and Darzynkiewicz, Z. (2001) Chromatin condensation and sensitivity of DNA in situ to denaturation during cell cycle and apoptosis — a confocal microscopy study. *Micron* **32**, 645–652 https://doi.org/10.1016/S0968-4328(00)00069-X
24 Choi, H., Hwang, J.-S. and Lee, D.G. (2014) Identification of a novel antimicrobial peptide, scolopendin 1, derived from centipede *Scolopendra subspinipes mutilans* and its antifungal mechanism. *Insect Mol. Biol.* **23**, 788–799 https://doi.org/10.1111/imb.12124
25 Dong, W., Mao, X., Guan, Y., Kang, Y. and Shang, D. (2017) Antimicrobial and anti-inflammatory activities of three chensinin-1 peptides containing mutation of glycine and histidine residues. *Sci. Rep.* **7**, 40228 https://doi.org/10.1038/srep40228
26 Lee, H., Woo, E.R. and Lee, D.G. (2016) (–)-Nortrachelogenin from *Partrinia scabiosaefolia* elicits an apoptotic response in *Candida albicans*. *FEMS Yeast Res.* **16**, 1–10 https://doi.org/10.1093/femsyr/fow013
27 Coyle, B., Kinsella, P., McCann, M., Devereux, M., O'Connor, R., Clynes, M. et al. (2004) Induction of apoptosis in yeast and mammalian cells by exposure to 1,10-phenanthroline metal complexes. *Toxicol. Vitr.* **18**, 63–70 https://doi.org/10.1016/j.tiv.2003.08.011
28 Perrone, G.G., Tan, S.X. and Dawes, I.W. (2008) Reactive oxygen species and yeast apoptosis. *Biochim. Biophys. Acta, Mol. Cell Res.* **1783**, 1354–1368 https://doi.org/10.1016/j.bbamcr.2008.01.023
29 Cai, J., Yang, J. and Jones, D.P. (1998) Mitochondrial control of apoptosis: the role of cytochrome *c*. *Biochim. Biophys. Acta* **1366**, 139–149 PMID:9714780
30 Khan, A., Ahmad, A., Khan, L.A. and Manzoor, N. (2014) *Ocimum sanctum* (L.) essential oil and its lead molecules induce apoptosis in *Candida albicans*. *Res. Microbiol.* **165**, 411–419 https://doi.org/10.1016/j.resmic.2014.05.031
31 Brookes, P.S., Yoon, Y., Robotham, J.L., Anders, M.W. and Sheu, S.S. (2004) Calcium, ATP, and ROS: a mitochondrial love-hate triangle. *Am. J. Physiol. Cell. Physiol.* **287**, C817–C833 https://doi.org/10.1152/ajpcell.00139.2004
32 Carraro, M. and Bernardi, P. (2016) Calcium and reactive oxygen species in regulation of the mitochondrial permeability transition and of programmed cell death in yeast. *Cell Calcium* **60**, 102–107 https://doi.org/10.1016/j.ceca.2016.03.005
33 Yao, G., Yang, L., Hu, Y., Liang, J., Liang, J. and Hou, Y. (2006) Nonylphenol-induced thymocyte apoptosis involved caspase-3 activation and mitochondrial depolarization. *Mol. Immunol.* **43**, 915–926 https://doi.org/10.1016/j.molimm.2005.06.031
34 Wang, Y., Chen, C.H., Hu, D., Ulmschneider, M.B. and Ulmschneider, J.P. (2016) Spontaneous formation of structurally diverse membrane channel architectures from a single antimicrobial peptide. *Nat. Commun.* **7**, 13535 https://doi.org/10.1038/ncomms13535
35 Choi, H., Hwang, J.-S. and Lee, D.G. (2013) Antifungal effect and pore-forming action of lactoferricin B like peptide derived from centipede *Scolopendra subspinipes mutilans*. *Biochim. Biophys. Acta* **1828**, 2745–2750 https://doi.org/10.1016/j.bbamem.2013.07.021
36 Zamora-Carreras, H., Strandberg, E., Mühlhäuser, P., Bürck, J., Wadhwani, P., Jiménez, M.Á. et al. (2016) Alanine scan and (2)H NMR analysis of the membrane-active peptide BP100 point to a distinct carpet mechanism of action. *Biochim. Biophys. Acta* **1858**, 1328–1338 https://doi.org/10.1016/j.bbamem.2016.03.014
37 Rautenbach, M., Troskie, A.M. and Vosloo, J.A. (2016) Antifungal peptides: to be or not to be membrane active. *Biochimie* **130**, 132–145 https://doi.org/10.1016/j.biochi.2016.05.013
38 Lv, Y., Wang, J., Gao, H., Wang, Z., Dong, N., Ma, Q. et al. (2014) Antimicrobial properties and membrane-active mechanism of a potential α-helical antimicrobial derived from cathelicidin PMAP-36. *PLoS ONE* **9**, e86364 https://doi.org/10.1371/journal.pone.0086364
39 Ly, J.D., Grubb, D.R. and Lawen, A. (2003) The mitochondrial membrane potential ($\Delta\psi$m) in apoptosis: an update. *Apoptosis* **8**, 115–128 PMID:12766472
40 Corral, M.J., Benito-Peña, E., Jiménez-Antón, M.D., Cuevas, L., Moreno-Bondi, M.C. and Alunda, J.M. (2016) Allicin induces calcium and mitochondrial dysregulation causing necrotic death in leishmania. *PLoS Negl. Trop. Dis.* **10**, e0004525 https://doi.org/10.1371/journal.pntd.0004525
41 Pereira, C., Camougrand, N., Manon, S., Sousa, M.J. and Côrte-Real, M. (2007) ADP/ATP carrier is required for mitochondrial outer membrane permeabilization and cytochrome c release in yeast apoptosis. *Mol. Microbiol.* **66**, 571–582 https://doi.org/10.1111/j.1365-2958.2007.05926.x
42 Green, D.R. and Reed, J.C. (1998) Mitochondria and apoptosis. *Science* **281**, 1309–1312 PMID:9721092
43 Mustonen, P., Virtanen, J.A., Somerharju, P.J. and Kinnunen, P.K. (1987) Binding of cytochrome c to liposomes as revealed by the quenching of fluorescence from pyrene-labeled phospholipids. *Biochemistry* **26**, 2991–2997 PMID:3038173
44 Stepanov, G., Gnedenko, O., Mol'nar, A., Ivanov, A., Vladimirov, Y. and Osipov, A. (2009) Evaluation of cytochrome c affinity to anionic phospholipids by means of surface plasmon resonance. *FEBS Lett.* **583**, 97–100 https://doi.org/10.1016/j.febslet.2008.11.029

Biochemical Journal (2018) **475** 1385–1396
https://doi.org/10.1042/BCJ20170894

45 Rytömaa, M., Mustonen, P. and Kinnunen, P.K. (1992) Reversible, nonionic, and pH-dependent association of cytochrome c with cardiolipin-phosphatidylcholine liposomes. *J. Biol. Chem.* **267**, 22243–22248 PMID:1331048

46 Belikova, N.A., Vladimirov, Y.A., Osipov, A.N., Kapralov, A.A., Tyurin, V.A., Potapovich, M.V. et al. (2006) Peroxidase activity and structural transitions of cytochrome c bound to cardiolipin-containing membranes. *Biochemistry* **45**, 4998–5009 https://doi.org/10.1021/bi0525573

47 Kagan, V.E., Borisenko, G.G., Tyurina, Y.Y., Tyurin, V.A., Jiang, J., Potapovich, A.I. et al. (2004) Oxidative lipidomics of apoptosis: redox catalytic interactions of cytochrome c with cardiolipin and phosphatidylserine. *Free Radic. Biol. Med.* **37**, 1963–1985 https://doi.org/10.1016/j.freeradbiomed.2004.08.016

48 Díaz-Moreno, I., García-Heredia, J.M., Díaz-Quintana, A. and De la Rosa, M.A. (2011) Cytochrome c signalosome in mitochondria. *Eur. Biophys. J.* **40**, 1301–1315 https://doi.org/10.1007/s00249-011-0774-4

49 Lee, H. and Lee, D.G. (2017) Fungicide Bac8c triggers attenuation of mitochondrial homeostasis and caspase-dependent apoptotic death. *Biochimie* **133**, 80–86 https://doi.org/10.1016/j.biochi.2016.12.013

50 Cao, Y., Huang, S., Dai, B., Zhu, Z., Lu, H., Dong, L. et al. (2008) *Candida albicans* cells lacking CaMCA1-encoded metacaspase show resistance to oxidative stress-induced death and change in energy metabolism. *Fungal Genet. Biol.* **46**, 183–189 https://doi.org/10.1016/j.fgb..11.001

51 Sedelnikova, O.A., Redon, C.E., Dickey, J.S., Nakamura, A.J., Georgakilas, A.G. and Bonner, W.M. (2010) Role of oxidatively induced DNA lesions in human pathogenesis. *Mutat. Res.* **704**, 152–159 https://doi.org/10.1016/j.mrrev.2009.12.005

52 Sena, L.A. and Chandel, N.S. (2012) Physiological roles of mitochondrial reactive oxygen species. *Mol. Cell* **48**, 158–167 https://doi.org/10.1016/j.molcel.2012.09.025